Lab on a Chip

PAPER

Cite this: *Lab Chip*, 2020, **20**, 634

Multiparameter urine analysis for quantitative bladder cancer surveillance of orthotopic xenografted mice†

Xiaotian Tan, ‡[a] Luke J. Broses,‡[bc] Menglian Zhou,[a] Kathleen C. Day,[bc] Wenyi Liu,[a] Ziqi Li,[a] Alon Z. Weizer,[bc] Katherine A. Munson,[bc] Maung Kyaw Khaing Oo,[d] Mark L. Day*[bc] and Xudong Fan *[a]

The human-derived orthotopic xenograft mouse model is an effective platform for performing *in vivo* bladder cancer studies to examine tumor development, metastasis, and therapeutic effects of drugs. To date, the surveillance of tumor progression in real time for orthotopic bladder xenografts is highly dependent on semi-quantitative *in vivo* imaging technologies such as bioluminescence. While these imaging technologies can estimate tumor progression, they are burdened with requirements such as anesthetics, specialized equipment, and genetic modification of the injected cell line. Thus, a convenient and non-invasive technology to quantitatively monitor the growth of bladder cancer in orthotopic xenografts is highly desired. In this work, using a microfluidic chemiluminescent ELISA platform, we have successfully developed a rapid, multiparameter urine-based and non-invasive biomolecular prognostic technology for orthotopic bladder cancer xenografts. This method consists of two steps. First, the concentrations of a panel of four urinary biomarkers are quantified from the urine of mice bearing orthotopic bladder xenografts. Second, machine learning and principal component analysis (PCA) algorithms are applied to analyze the urinary biomarkers, and subsequently, a score is assigned to indicate the tumor growth. With this methodology, we have quantitatively monitored the orthotopic growth of human bladder cancer that was inoculated with low, medium, and high cancer cell numbers. We also employed this method and performed a proof of principle experiment to examine the *in vivo* therapeutic efficacy of the EGFR inhibitor, dacomitinib.

Received 10th October 2019,
Accepted 20th December 2019

DOI: 10.1039/c9lc01006h

rsc.li/loc

Introduction

Bladder cancer is the sixth most common malignant tumor in the United States and is one of the most widespread carcinomas globally.[1,2] To study tumor progression, invasion mechanisms, and therapeutic strategies for invasive bladder cancers in humans, biologically relevant mouse models of cancer have been developed including carcinogen-based,[3,4] genetically engineered,[5] and human-derived xenografts.[6] The human-derived orthotopic xenograft model is believed to have high clinical relevance because of its high throughput, low cost, and high similarity to cancer found in patients.[6] In our most-updated approach, bladder cancer cell lines are directly inoculated into the bladder lumen of NSG (NOD *scid* gamma) mice[7] where they rapidly seed into the urothelial lining.[6] Consequently, tumors can develop quickly in the mouse bladder environment.

The surveillance of tumor progression in all human-derived orthotopic bladder xenografts still highly depends on either end-point pathological and immunohistochemical analyses, or *in vivo* imaging technologies such as PET–CT (positron emission tomography–computed tomography),[8,9] MRI (magnetic resonance imaging),[10] ultrasound imaging,[11] and bioluminescence imaging.[12,13] However, end-point histological analyses cannot provide real-time information regarding tumor progression. The real-time *in vivo* imaging approaches, while being able to estimate the tumor size during growth, require expensive equipment, highly skilled personnel, time-consuming steps, imaging agents, hair removal, and/or anesthetics, and are limited by the device capacity to process a large number of mice.[14] More importantly, these *in vivo* imaging approaches generally

[a] *Department of Biomedical Engineering, University of Michigan, Ann Arbor, MI 48109, USA. E-mail: xsfan@umich.edu*
[b] *Department of Urology, University of Michigan, Ann Arbor, MI 48109, USA. E-mail: mday@umich.edu*
[c] *Rogel Comprehensive Cancer Center, University of Michigan, Ann Arbor, MI 48109, USA*
[d] *Optofluidic Bioassay, LLC, 674 S. Wagner Rd., Ann Arbor, MI 48103, USA*
† Electronic supplementary information (ESI) available. See DOI: 10.1039/c9lc01006h
‡ Equally Contribution.

cannot provide any biomolecular information about the tumor. As one of the most commonly used approaches for tumor surveillance in animal models, bioluminescence intensity may provide only semi-quantitative information about the tumor size. In addition, since genetically modified-cell lines are needed, it may be difficult to extend bioluminescence imaging approaches to other types of animal models (*e.g.*, carcinogen induced cancer models). Thus, a broadly applicable, convenient, and non-invasive technology is highly desired to quantitatively monitor the progression of orthotopically implanted human tumor xenografts.

Urine carries a vast amount of cellular and biomolecular information related to urinary diseases.[15,16] It has been found that urinary biomarkers can be used to provide diagnostic and prognostic information for human bladder cancers.[16–18] Therefore, detection of a panel of selected biomarkers in urine may provide a simple, cost-effective, and non-invasive means for tumor progression monitoring. However, the correlation between a panel of multiple urinary biomarkers and tumor progression in the orthotopic bladder cancer xenograft model has not been investigated. This is due in part to the limited analytical capability of the traditional ELISA (enzyme-linked immunosorbent assay) technology that is widely used in analyzing biomarkers in urine, but suffers from low sensitivity, long assay time (typically 4–6 hours), and large sample volumes (typically 50–100 μL per marker) which are difficult for a mouse to produce.[19]

Here, we developed a methodology that uses a panel of urinary protein biomarkers to quantitatively monitor tumor growth in live orthotopic xenograft bearing mice. This method consists of a two-step approach. First, the concentrations of urinary biomarkers are quantified. Then, machine learning and principal component analysis (PCA) algorithms[20] are applied to analyze the urinary biomarkers, and subsequently, a score is assigned to indicate the tumor growth. More specifically, in this work, we used three groups of mice injected with low, medium, and high numbers of human-derived bladder cancer cells (UM-UC-5 cell line[21]) as the model system. Four protein bladder cancer biomarkers with high clinical or pathological significance were selected as a panel that included EGFR,[22,23] HER2,[24,25] ADAM15,[26,27] and Survivin.[18,28] The biomarkers in the mouse urine were analyzed every week for four weeks using an automated microfluidic ELISA technology and the associated protocols developed in-house, which is able to rapidly and sensitively detect those biomarkers with only 8 μL of sample per marker and a detection limit down to a single-digit pico-gram per mL.[29] Then machine learning and PCA were performed with our 4-marker results, which revealed that the distribution of the PCA data points correlates well with the bioluminescence imaging readings about the tumor burden. Mice with small tumors can be distinguished easily from those with large tumors. The tumor burden can be further quantified with a "tumor growth score" that is calculated based on the PCA results. Finally, our method was employed to study the *in vivo* therapeutic efficacy of an anti-tumor drug, dacomitinib, in the orthotopic xenograft mouse model.

Experimental

1. Workflow

We designed a series of experiments to demonstrate the feasibility and to validate our method of urine-based tumor growth analysis. Various numbers of human-derived bladder cancer cells (UM-UC-5 cell line) were injected into the bladder lumens of NSG mice as previously described in ref. 6 (see (Fig. 1) for illustration). The UM-UC-5 cell line was previously engineered to express firefly luciferase and is capable of being used with luciferin-based bioluminescence imaging. The UM-UC-5 bladder tumor progresses gradually over a four week surveillance period (spontaneous muscle invasion was observed by the end of the study). 50–80 μL of urine per mouse was collected once per week. The urinary concentrations for a panel of bladder cancer biomarkers were quantified *via* microfluidic ELISA. Using the concentration data of these biomarkers, a PCA analysis and subsequent score assigning was performed. To establish a correlation between the urinary "tumor growth score" and the actual tumor severity, we also performed concurrent tumor surveillance with traditional qualitative or semi-quantitative technologies such as endpoint histological analysis and weekly *in vivo* bioluminescent imaging (technology validation assays).

We selected four urinary biomarkers that are believed to be either strongly involved in tumor growth, muscle invasion or have high clinical relevance for cancer diagnostics. They are EGFR,[22,23] HER2,[24,25] ADAM15,[26,27] and Survivin,[15,16,28] which are expressed in a large number of human bladder cancer cell lines. As reported in previously, the expression levels of all genes in the UM-UC-5 cell line was evaluated through mRNA sequencing.[30] Based on the mRNA expression data, the UM-UC-5 cell line was determined to has highly amplified expression of EGFR, normal-level expression of HER2 (*ERBB2* gene) and ADAM15, and relatively low expression of Survivin (*BIRC5* gene).[30] The protein expression of these markers were verified in the whole cell lysates of several bladder cancer cell lines through western blot (Fig. S1†). Since the UM-UC-5 cell line was collected from a female patient and has more consistent growth in the bladders of female mice, we chose to conduct this experiment with female NSG mice.

2. Microfluidic chemiluminescent ELISA

Having an accurate and sensitive biomarker quantification technology is critical to building a reliable tumor growth model that relies solely on urinary biomarker measurements. Although widely used in protein quantification, the traditional 96-well plate based ELISA is not capable of doing such measurements due to its large sample consumption per marker (50–100 μL) and limited sensitivity.[19] The

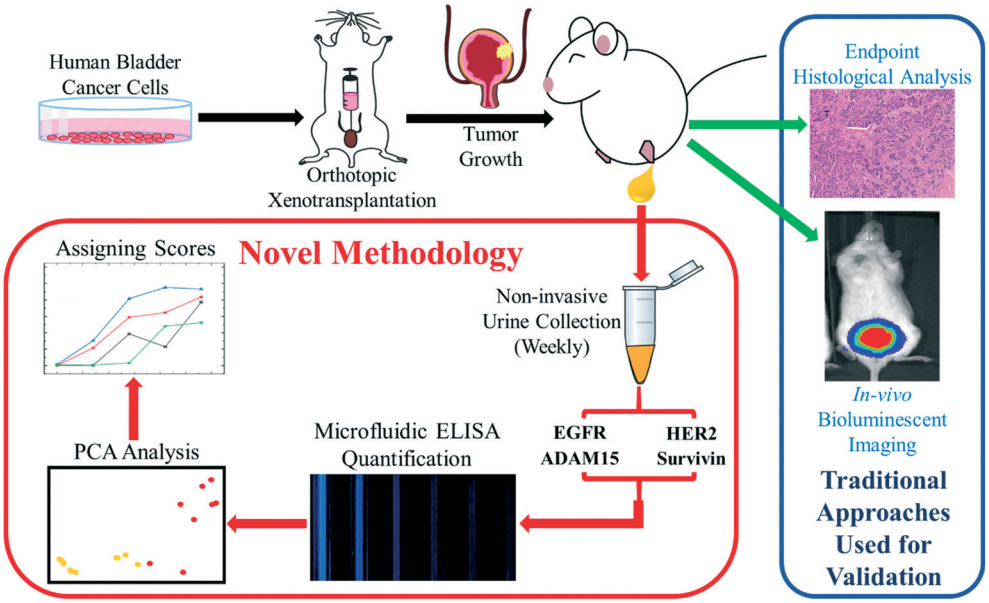

Fig. 1 Illustration of the workflow. Bladder cancer was induced by injecting human-derived bladder cancer cells (UM-UC-5) into the bladders of immunodeficient mice. The tumor progresses in a 4 week period, during which, at least 50 μL of urine was collected once per week. A panel of four protein bladder cancer biomarkers (EGFR, HER2, ADAM15, and Survivin) in urine were selected to build the tumor growth model. An automated microfluidic chemiluminescent ELISA system and associated detection protocol developed in-house, which could complete an assay in about 45 minutes with only 8 μL of sample (per biomarker) and a detection limit down to a few pico-grams per mL, were employed to quantify the biomarkers' concentrations in urine weekly. Principal component analysis (PCA) was used to analyze the ELISA results for the four biomarkers and subsequently establish a quantitative tumor growth model. Concurrently, endpoint histological analysis and weekly *in vivo* bioluminescent imaging were performed to validate the effectiveness and accuracy of our methodology.

limitation of the traditional ELISA exacerbates for mouse urine (typically only 50–80 μL can be collected each time). Since the urinary concentrations of those biomarkers are expected to be low, a high-power dilution is not practically applicable.

In this work, we employed microfluidic chemiluminescent ELISA technology developed in-house, which has much higher sensitivities and requires much smaller sample volumes (only 8 μL per biomarker) than the traditional 96-well plate based ELISA. Detailed description of the microfluidic chemiluminescent ELISA and the disposable 12-channel cartridge can be found in our previous publication.[29] In addition, we employed streptavidin poly-HRP instead of standard streptavidin-HRP to amplify the chemiluminescent signal.[31,32] Meanwhile, the corresponding blocking protocol was developed to suppress non-specific adsorption of poly-HRP to the sensor surface.[33] As a result, the signal-to-noise ratio was increased 5-fold over the previous protocol (Fig. S2†). Excluding the sensor preparation (*i.e.*, capture antibody immobilization, which is usually done en-masse well in advance), the total assay time was about 45 minutes (Fig. 2(A)), much shorter than 4–5 hours usually used in 96-well-plate based ELISA.

We established calibration curves for the four bladder cancer biomarkers (Fig. 2(C)–(F)). The linear dynamic ranges in the log–log scale are 3–2000 pg mL^{-1}, 3–2000 pg mL^{-1}, 5–4000 pg mL^{-1}, and 8–6000 pg mL^{-1} for EGFR, HER2, ADAM15, and Survivin, respectively (the lower LOD is calculated by background +2.5σ), which cover approximately three orders of magnitude. The intra-assay variance is close to or smaller than 10% (Fig. S3†). In contrast, the dynamic ranges with plate based ELISA (from user's manual of the kits) are 31–2000 pg mL^{-1}, 55–3500 pg mL^{-1}, 63–4000 pg mL^{-1}, and 63–4000 pg mL^{-1} for EGFR, HER2, ADAM15, and Survivin, respectively.[34–37] The calibration curves demonstrated significantly improved sensitivity over traditional plate-based ELISA, even with the same antibodies. The performance introduced above can fully support the detection ranges that were used in the actual urine measurements, *i.e.*, 10–2000 pg mL^{-1} for EGFR, 10–2000 pg mL^{-1} for HER2, 10–4000 pg mL^{-1} for ADAM15, and 10–4000 pg mL^{-1} for Survivin. To ensure the measurement reliability, the lower ends of the dynamic ranges (below 10 pg mL^{-1}) were not used for actual urine measurements and were marked as 0 pg mL^{-1}.

Results

1. Converting the ELISA measurements to a PCA model

With the microfluidic chemiluminescent ELISA technology described in section 2, we performed the actual animal studies and converted the urinary biomarker results into a PCA model. We injected a group of mice with a low number of UM-UC-5 cells (marked as low number group), along with a tumor-free control group. Those mice serve as the "training set" for the subsequent studies using medium and high UM-

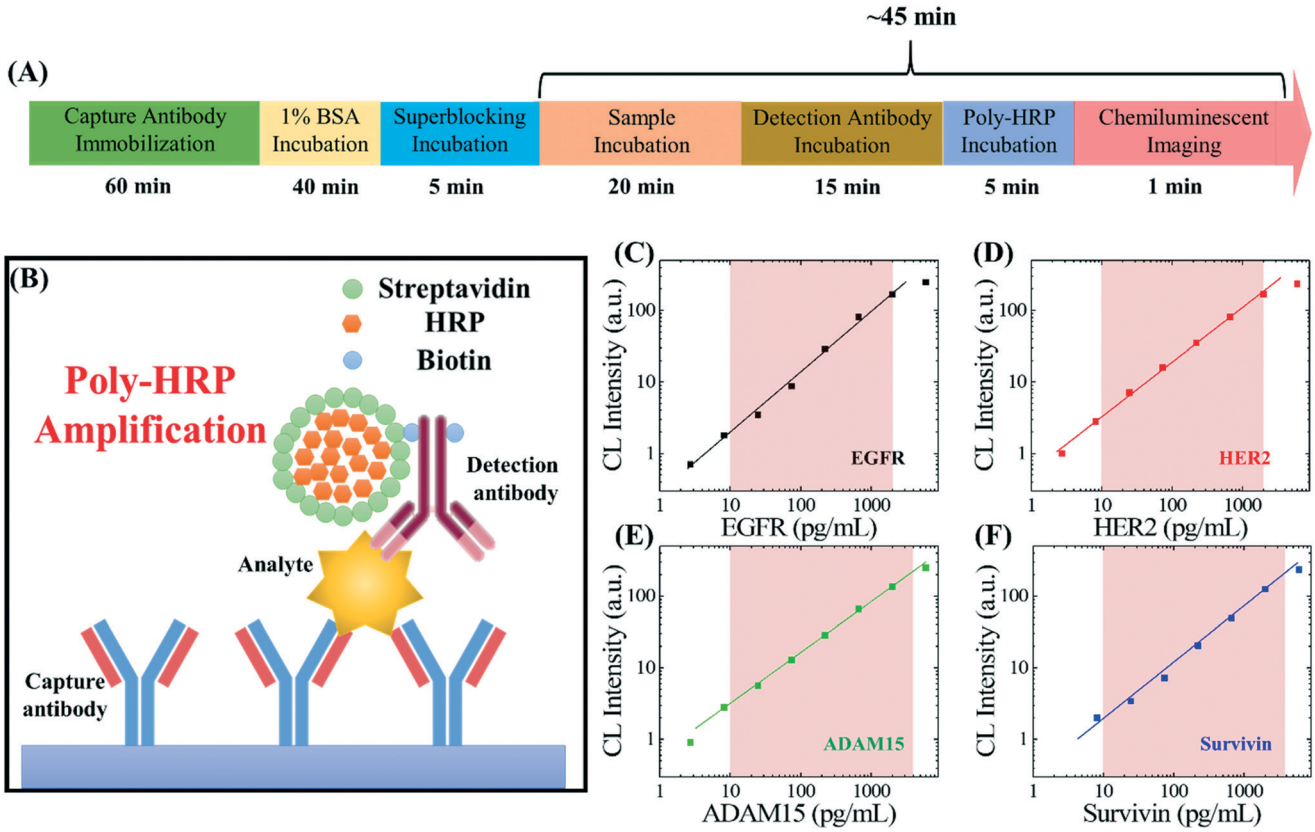

Fig. 2 The highly-sensitive microfluidic chemiluminescent ELISA. (A) ELISA assay protocol for the four bladder cancer biomarkers. The first 105 minutes were used for ELISA sensor preparation (*i.e.*, capture antibody immobilization), which is usually done well in advance. The actual assay time was about 45 minutes, including a rinsing step (with 0.05% Tween) after each incubation step. (B) Illustration of the sandwich ELISA assay with poly-HRP amplification. The use of poly-HRP enhances the signal approximately five-fold, compared to regular HRP conjugated on the detection antibody. (C)–(F) Calibration curves for the four biomarkers with our microfluidic chemiluminescent ELISA. The dynamic range for all of the four biomarkers covers over three orders of magnitude. The respective LODs were 3 pg mL^{-1} for EGFR, 3 pg mL^{-1} for HER2, 5 pg mL^{-1} for ADAM15, and 8 pg mL^{-1} for Survivin (calculated by background +2.5σ). The shaded areas denote the ranges used in the actual urine measurements, *i.e.*, 10–2000 pg mL^{-1} for EGFR, 10–2000 pg mL^{-1} for HER2, 10–4000 pg mL^{-1} for ADAM15, and 10–4000 pg mL^{-1} for Survivin. The solid lines are the linear fit in the log–log scale, within their dynamic ranges.

UC-5 cell numbers. To be specific, 0.5 million UM-UC-5 bladder cancer cells were injected into the bladder lumens of the four experimental mice (L1–L4) on day 0. For the sham (control) mouse, a buffer solution without cells was injected into one sham mouse (Fig. 3). The urinary concentrations were measured for the four biomarkers at different time points after tumor inoculation (Fig. 3(A)–(D)). Note that for EGFR measurements, the urine samples were diluted three times with 1% BSA in PBS. For HER2, ADAM15, and Survivin measurements, the urine samples were diluted two times with 1% BSA in PBS. As presented in Fig. 3(A)–(D), the urinary concentrations of the biomarkers generally have increasing trends with some fluctuations. Due to 3% cross-reactivity between human EGFR and mouse EGFR (according to the ELISA kit's user manual) there were some background readings for EGFR, even before the tumor inoculation. The typical background readings at week 0 for EGFR (equivalent human EGFR concentration) were between 200 and 1000 pg mL^{-1}. The "plateau" in the EGFR readouts was resultant from measurement that exceeded the upper limit of detection. All measurements that exceeded the detection limit were marked as the upper LOD (2000 × 3 = 6000 pg mL^{-1}). For HER2 and ADAM15, no background signal was observed at week 0 and the urinary concentration readouts increased from nearly 0 pg mL^{-1} to 50–400 pg mL^{-1} by the end of week 4. For Survivin, no background signal was observed at week 0, but due to the relatively low protein expression level, low readouts (<100 pg mL^{-1}) were observed from two of the four mice in the following weeks. The increase in urinary biomarker concentrations is typically higher than two orders of magnitude (especially for HER2, ADAM15, and Survivin), which suggests that a creatinine-based urine concentration normalization is not necessarily required (the distribution of creatinine levels for all samples is within an order of magnitude, see Fig. S4†).

PCA analysis was performed with the biomarker concentration data collected from the ELISA measurements (Fig. 3(E)). The data points from the mice with lower bioluminescence readouts (<1 × 10^8) were represented by yellow dots and the data points from mice with higher bioluminescence readings (>1 × 10^8) were represented by red dots. The data points were clustered into two distinct groups,

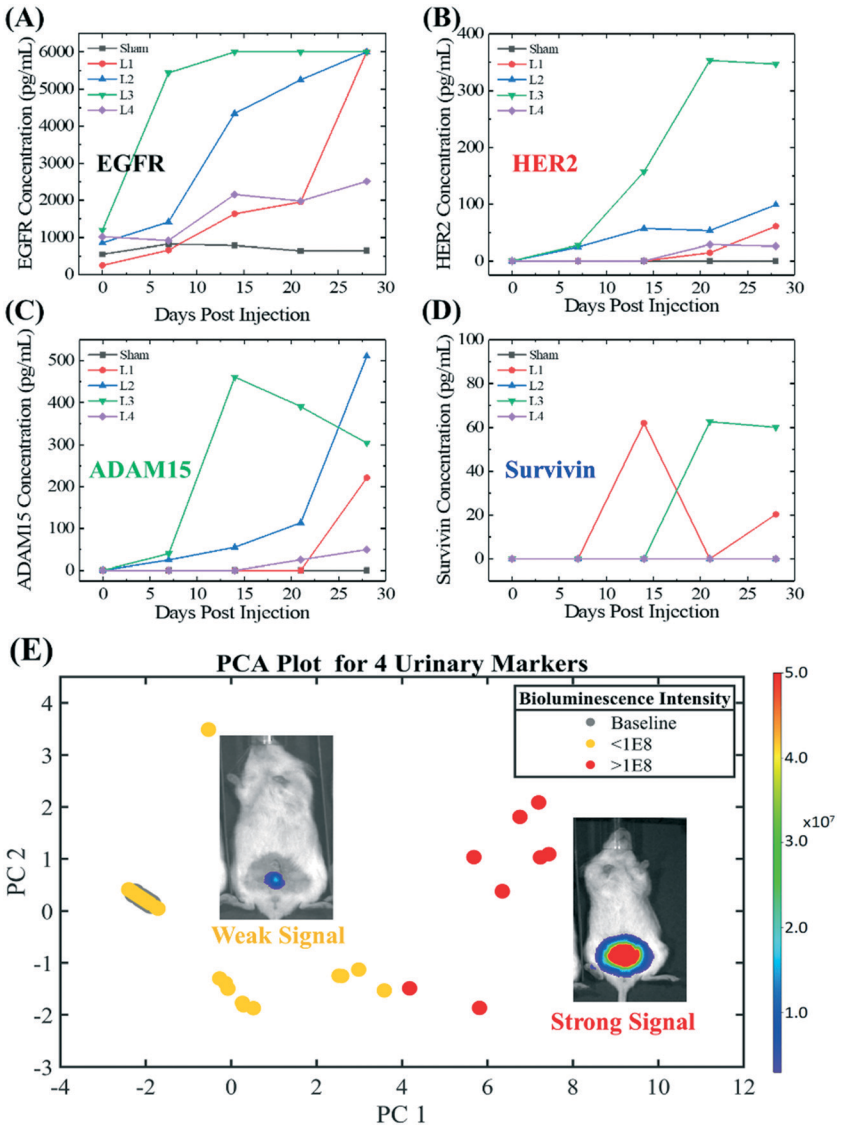

Fig. 3 Converting urinary biomarker concentrations to a PCA model. (A)–(D) Urinary concentrations of the four biomarkers in five mice over 4 weeks. A low number of 0.5 million UM-UC-5 (luciferase positive) bladder cancer cells were injected into the bladder lumens of the four experimental mice (L1–L4) on day 0. Buffer solution without cells was injected into the sham mice. The "plateau" in the EGFR readouts was caused by the measurement that exceeded the upper limit of the detection range. (E) PCA plot generated based on the urinary biomarker concentrations in (A)–(D). The distribution of the data points correlates well with the bioluminescent imaging readings (see the insets for example) about the tumor size (see the scale bar for the correlation between colors and bioluminescent intensities). The mice used here serve as the training set for all subsequent experiments and PCA analyses. The corresponding calculation algorithms will be used to analyze data in the remaining "testing" sets of experiments. Note that the baseline is clustered around the coordinates (−2, 0.2) on the PCA plot.

which means that the urine-based PCA results correlates well with the bioluminescence imaging readings about the tumor load (see the insets for example). The PC1 and PC2 components account for 84.1% and 9.0% of the variability (weights), respectively. The eigenvalues were calculated for all four PC scores (Fig. S5†). The baseline data points (before the tumor was injected and the sham animal) are all clustered around (−2, 0.2). The data points that correlate with the mice with high bioluminescence intensity readouts ($>1 \times 10^8$) are all distributed in the right half of this two-dimensional plot (*i.e.*, PC1 $>$ 4). Most importantly, the mice with relatively low bioluminescence intensity readouts can be easily distinguished from the mice with relatively high bioluminescence intensity readouts.

2. Testing sets

After successfully modeling the training set (*i.e.*, the mice injected with a low number of initial cancer cells) with PCA, we investigated two more groups of mice with a medium number (1 million) and a high number (1.5 million) of UM-UC-5 cancer cells injected into mouse bladders, which serve as the testing sets. Same as the training set, urine was collected weekly and the urinary biomarker concentrations

were quantified *via* microfluidic chemiluminescent ELISA (Fig. S6 and S7†).

The PCA results from these two groups were generated with the same algorithm and parameters that were used for PCA analysis of the training set. We included trajectories on the PCA plots for individual animals in order to visualize tumor growth (Fig. 4). Similar to the training set, the trajectories for the testing sets all started from the baseline region around (−2, 0.2) in the PCA plot and progressed towards the large tumor region denoted by the red shaded area. Note that mouse M1, H1 and H3 died before the 4 week post-tumor-injection endpoint. The similarities between the PCA results in the training set and the testing sets suggest that this tumor growth model is valid over a range of injected UM-UC-5 cancer cell numbers (0.5–1.5 million).

3. Quantifying tumor growth with a urine-based "tumor growth score"

To provide a direct and quantitative assessment of tumor growth, this two-dimensional PCA model is subsequently transformed into a one-dimensional evaluation system – "tumor growth score", which is calculated as the distance between a particular point in the PCA plot and the averaged baseline point centered around (−2, 0.2) (Fig. S8†). The tumor growth scores were calculated for mice with low, medium, and high injected cell quantities at each time point (Fig. 5(A)–(C)).

During the four weeks of tumor growth, the scores from the mice in all three groups show clear increasing trends (increased from around 0 to a range between 5 and 12). The slopes for the "low number" group are the lowest among the

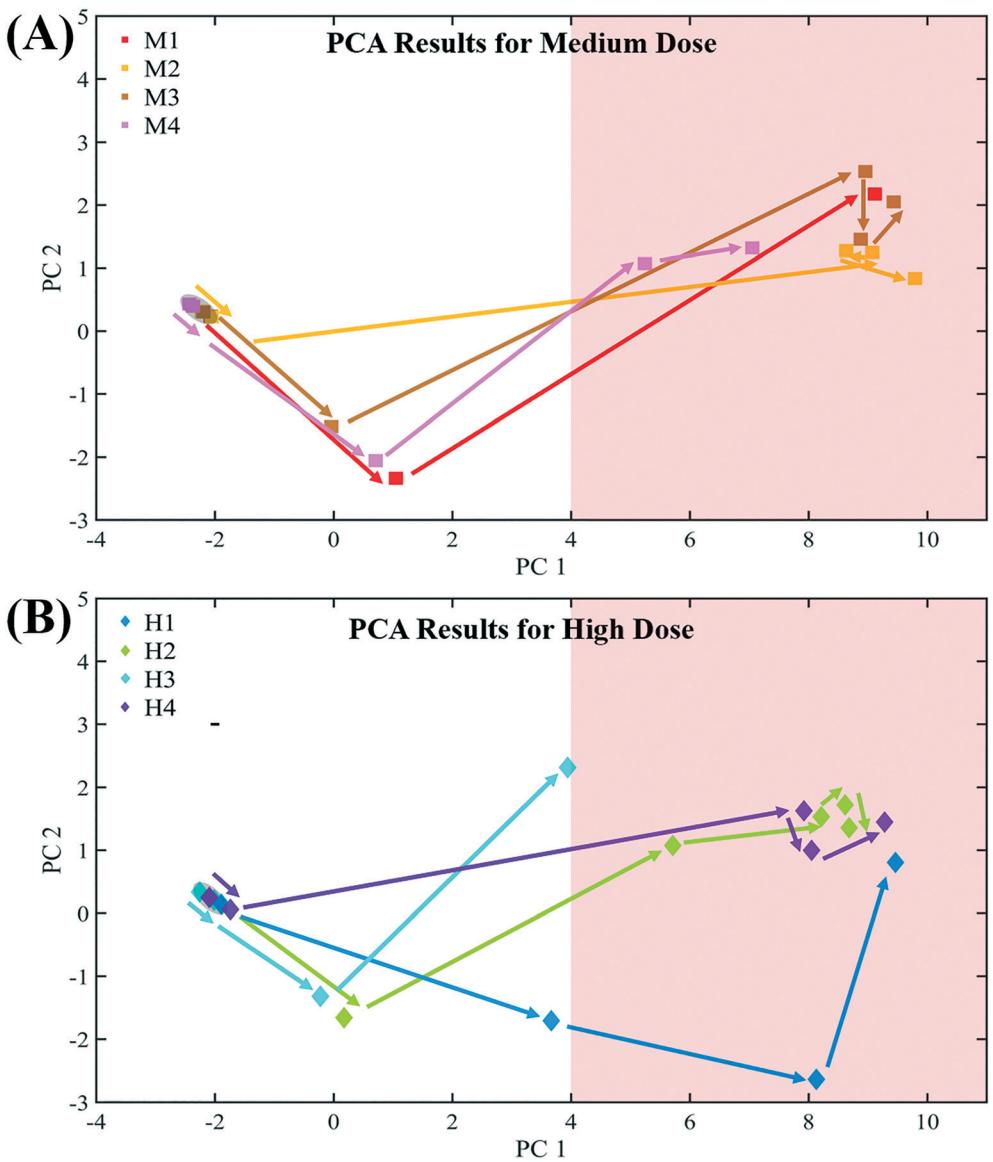

Fig. 4 Trajectories of the mice on a PCA plots indicated by arrows during the 4 week urine measurements. These mice were injected with a medium number of 1 million UM-UC-5 cells (A) and a high number of 1.5 million UM-UC-5 cells (B) and they serve as the testing sets using the PCA parameters obtained in Fig. 3(E). They all started from the baseline around (−2, 0.2) on the PCA plot and progressed towards the large tumor region denoted by the shaded area. Note that mouse M1, H1 and H3 were euthanized before the 4 week end point due to tumor burden.

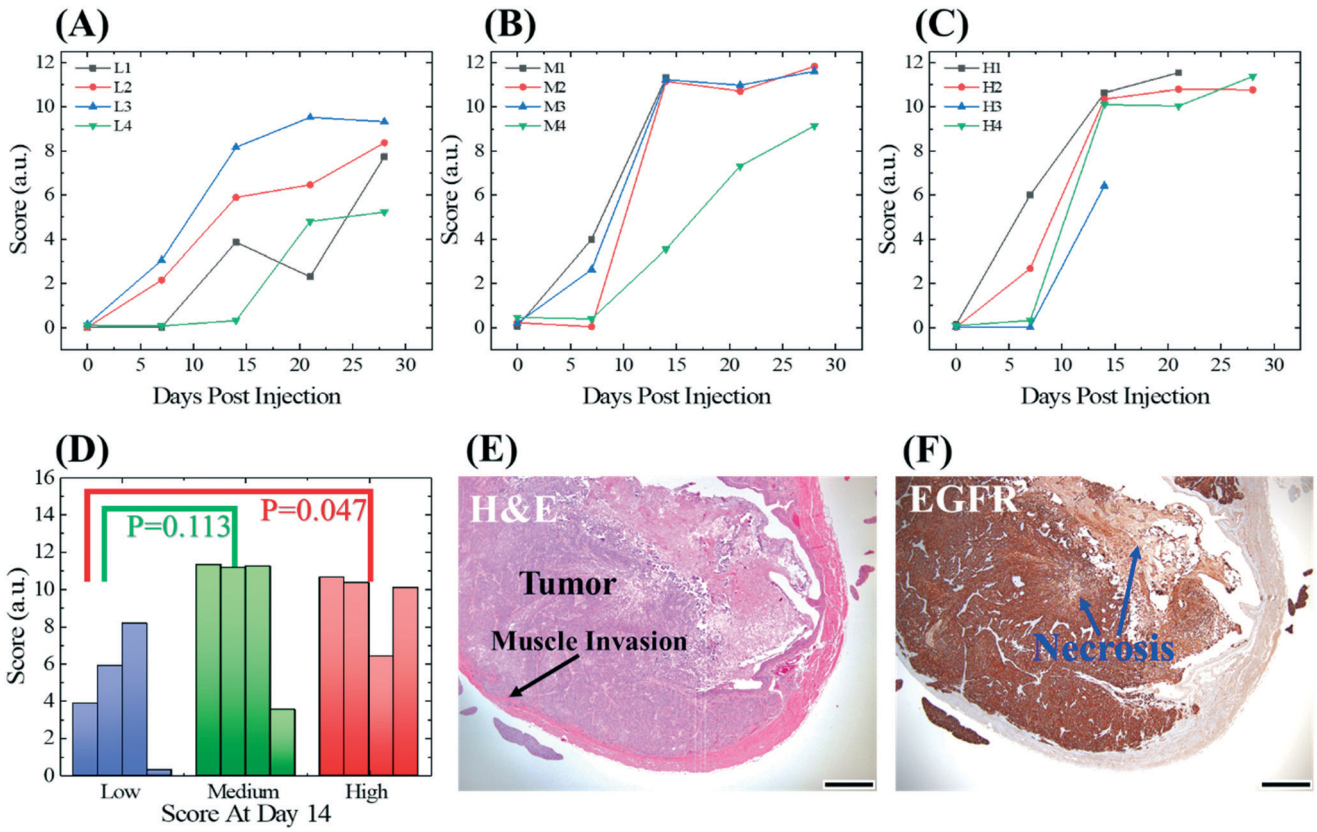

Fig. 5 Quantifying tumor growth with PCA scores and endpoint histology. (A)–(C) Quantification of tumor growth using the scores obtained on the PCA plot for low, medium, and high numbers of initially injected of UM-UC-5 cells. (D) Comparison of the scores on day 14 for the mice that had received low, medium, and high initial cancer cell numbers. (E) and (F) Endpoint histological slides with H&E staining and EGFR immunohistochemistry staining for a representative "large" orthotopic bladder xenograft. Muscle invasion can be found at the bottom left corner of the cross-sectional image, as marked by the arrow. Tumors at this stage usually have relatively low surface-to-volume ratios and multiple necrotic centers. The scale bars stand for 0.5 mm.

three groups. In addition, lower initial cancer cell numbers are beneficial for the mouse's survival with tumor as deaths were observed in both the medium and high number groups before study completion. The increasing trend of the score for the first week may not be very significant for half of the mice (6 out of 12) but the score for the second week are significantly higher than the baseline points for all mice (p = 0.037, 0.003, and 0.00008 for low, medium, and high number groups, respectively). This indicates that although the initially injected UM-UC-5 cell quantities are the same for all mice within each group, the uptake rates for the cancer cells may be significantly different from mouse to mouse. The scores for most of the mice reached "plateaus" after the second week in the medium and high number groups. Therefore, a comparison was performed between the scores for each group at the second week (Fig. 5(D)). The scores from the high number group have statistically significant differences from those from the low number group (p = 0.047). The scores from the medium number group were also higher than the scores for the low number group but the differences do not have statistical significance (p = 0.113) (due to the outlier M4). The scores from the medium and high number groups appear to be very similar (p = 0.974). This demonstrates that our "tumor growth score" can quantitatively reflect the orthotopic growth of the inoculated tumors, until they reach a very severe stage.

The "plateau" that appears in the medium and high number groups can be explained by the following conjecture. Once tumors fill the bladder lumen, the surface-to-volume ratio becomes smaller and the tumor may grow outward impairing cellular diffusion within the bladder. After the tumors reach a certain volume, the center of the tumor may become necrotic due to a lack of nutrients. Both of these problems will inhibit the urinary concentration of the biomarkers from increasing. This hypothesis is supported by the endpoint histological slides where one representative mouse presented with a necrotic tumor (Fig. 5(E) and (F), collected from mouse L1). Tumors at this stage usually have relatively low surface-to-volume ratios and showed multiple necrotic areas (Fig. S9†).

4. *In vivo* dacomitinib therapeutic efficacy study

The UM-UC-5 cell line has an increased copy number of EGFR, which is a target of many anti-cancer therapeutics. Dacomitinib, as a second-generation irreversible inhibitor of

the EGFR family, was recently approved by US FDA for the therapy of EGFR positive metastatic non-small cell lung cancer.[38] The *in vitro* inhibitory efficacy of dacomitinib for human bladder cancer cell lines was studied and reported by our previous research.[21] UM-UC-5, along with other bladder cancer cell lines, appeared to be sensitive to dacomitinib treatment (IC_{50} <5 μM).[21] *In vivo* therapeutic efficacy tests for dacomitinib were also performed with UM-UC-6 and UM-UC-9 cell lines with conventional evaluation methodologies.[39] However, the *in vivo* therapeutic efficacy of dacomitinib in treating UM-UC-5 orthotopic xenografts have not yet been investigated.

With the establishment of this non-invasive and quantitative methodology for the surveillance of orthotopic tumor growth, we conducted a pilot experiment regarding the *in vivo* therapeutic efficacy of dacomitinib with a group of four animals. Half-a-million UM-UC-5 cells (the same number used in the low number group) were injected into four NSG mice (D1–D4) due to the relatively mild growth rate (Fig. 5). Dacomitinib was administered to the mice between the first week (day 7) and the fourth week (day 28). Nine doses of dacomitinib by oral gavage at approximately 15 mg kg^{-1} every other day during this three week treatment.

Weekly urine collection was performed for four weeks. The urinary biomarker concentrations were measured, the PCA model was applied, and the tumor growth scores were calculated for these four mice in the same manner as our earlier sets. The scores for these four animals were plotted together with the scores for the low number group and the sham control mouse. The scores for the mice in the dacomitinib group stopped increasing after day 7 which is when the treatment began (Fig. 6(A)). Although some fluctuation was observed for mouse D1, the scores for all of the mice in this group ended up at very low levels by the end of the experiment (day 28).

Side-by-side comparisons were performed for the scores on day 7 (before the dacomitinib treatment started) and day 28 (endpoint), between the dacomitinib group and the control group (low initial cancer cell number without drug treatment). As presented in Fig. 6(B), no significant difference can be observed for the scores on day 7 (p = 0.978). In contrast, by the end of the experiment the difference between the two groups became very large and significant (p = 0.0002), as shown in Fig. 6(C). The results of the urinary measurements indicate that the dacomitinib treatment was effective in this *in vivo* test. We also used traditional examination methods to weigh the bladders and perform IHC. The bladder weights were significantly lower in the dacomitinib treated group (Fig. 6(D) and (E)), which corroborates our PCA finding that dacomitinib was efficacious in this model. The mice that received dacomitinib treatment appeared to have smaller and less "dense" tumors when comparing the IHC from each group (Fig. S10†).

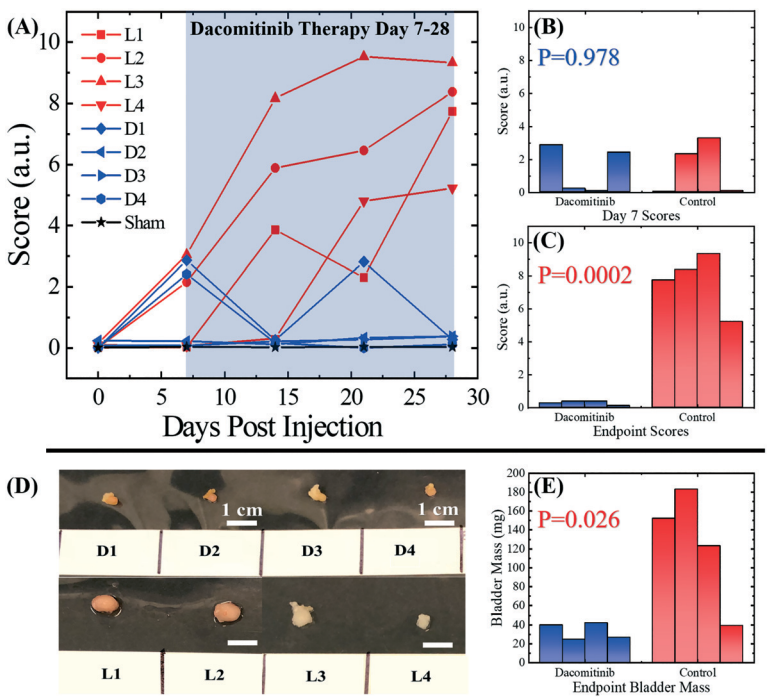

Fig. 6 Urine-based tumor growth quantification for an *in vivo* dacomitinib study. (A) Tumor growth scores for animals with (D1–D4) and without (L1–L4) dacomitinib treatment, between day 0 and day 28. Dacomitinib treatment was performed between day 7 and day 28. The scores for the sham mouse are also plotted. (B) Score comparison between the treated and control groups on day 7. No significant difference was observed. (C) Score comparison between treated and control groups on day 28. The scores from the control group were significantly higher than the dacomitinib treated group. (D) and (E) Result evaluation and validation. (D) The photos for the bladders with or without dacomitinib treatment. (E) Endpoint bladder mass comparison for both the dacomitinib treated and control groups.

Discussion

In this work, we have successfully developed a non-invasive, multiparameter urine-based biomolecular prognostic technology for bladder cancer orthotopic xenograft mouse model, which provides an alternative tumor surveillance approach for the labs that do not have access to those *in vivo* imaging facilities or skilled personnel (for bioluminescence imaging, PET–CT, MRI, ultrasound). While developing this method, we quantitatively monitored the growth of orthotopic bladder cancer xenografts that were induced by different initial cancer cell numbers across a four week period. We also conducted a pilot experiment that utilized this method for real-time surveillance of the *in vivo* therapeutic efficacy of dacomitinib.

Our results indicate that the model, built with multiple biomarkers, will lead to several unique advantages over single-parameter models. First, the background readings (noise) for a single biomarker (caused by cross-reactivity) were greatly reduced or even eliminated (see Fig. S11† for tumor growth scores with EGFR only and EGFR + HER2). Second, the saturation in a single biomarker's measurement will not stop the progression in the model as the increment in the readings of other biomarkers will dominate the progression in the model. Third, the selection of biomarkers with significantly different expression levels makes this modeling methodology broadly applicable to other human bladder cancer cell lines. For example, the four markers used in this study were proved to be expressed in a large number of human bladder cancer cell lines. While Survivin expression is relatively low in the current cell line (UM-UC-5), it is highly expressed in some other bladder cancer cell lines such as UM-UC-6. Certainly, recalibration of the biomarker selection may be necessary depending on the protein expression patterns of the desired cell line, but this is easily performed. It should be noted that, as a proof-of concept study, we did not aim to include all markers involved in bladder cancer's progression and invasion. Incorporating additional markers (*e.g.*, FGFR3, EpCAM, and CXCL1 for tumor growth and muscle invasion) may be potentially beneficial for the generalization of our model and approach.[40–43]

The development of this methodology also facilitated the optimization of the number of cancer cells for orthotopic injection. As the scores presented in Fig. 5(A)–(C), out of the three initial cancer cell numbers that were tested in this study, the "low number" group appears to have the shallowest increasing trend of tumor growth scores out of the three groups (while having a large endpoint tumor size) which is an essential for an animal model that is expecting to have a long survival time after tumor inoculation. The variation in tumor growth rates that were caused by different initial numbers of UM-UC-5 cells was observed and reported for the first time because such optimization is difficult to perform without a reliable quantitative tumor surveillance technology.

In addition to the animal model itself, our work also demonstrated strong potential in facilitating *in vivo* drug efficacy modeling in live animals. With our methodology, the necessity of luciferase transfection for patient-derived tumor cell lines can be reduced. This is especially beneficial for researches with patient-derived-xenograft models, as the tumor growth can be monitored through urine measurements. It can ultimately lead to an enhancement in the throughput for and cost performance in personalized precision medicine therapies in clinical settings.

With all the aforementioned features, the same modeling concept can easily be applied to other bladder cancer cell lines and adapted for other types of bladder cancer animal models. Carcinogen-based mouse models, syngeneic models, and PDX models,[44,45] could all benefit from a new approach to quantifying tumor burden in mice. Furthermore, this urine-based methodology should be applicable to research with other types of urinary system carcinomas, such as renal cell carcinoma and prostatic carcinoma.[46–49]

Although we have demonstrated very promising results for the surveillance of orthotopic tumor growth, there are many avenues for this method to progress. The trends for the urine measurements shortly after the introduction of dacomitinib are still unknown. To find out the exact "bifurcation point" between the treated and control groups, more data points can be added between week one and week two. Such intensified data points are also beneficial for investigating the tumor growth rate during the earlier stages of xenograft development.

As mentioned in the "Result" section, the change in biomarker concentrations was typically higher than two orders of magnitudes, thus the necessity for performing creatinine-based urine concentration normalization was reduced. However, such normalization may still be helpful for the measurements with the urine collected from animals with larger tumors because their urine generally appeared to be more diluted (caused by unknown reasons). Such normalization will likely make the "plateau" levels in the score shift to higher values and appear at later time points.

According to our previous research, local muscle invasion and distant metastasis typically occur by the fourth week and such metastasis was also observed by bioluminescence in these experiments (Fig. S11†). However, our current urine-based model is not capable of quantitatively monitoring the tumor invasion or metastasis after the tumors grow over the entire inner surface of the bladder. This limitation may be addressed by introducing more metastasis and invasion-related urinary markers (including protein, exosome, and micro-RNA markers) into this model.[50–56]

Materials & methods

Cell lines

The UM-UC-5, UM-UC-15, and UM-UC-18 cell lines were obtained from their originator, Dr. H. Barton Grossman of the MD Anderson Cancer Center (Houston, TX). Cells were cultured in Dulbecco's modified Eagle medium (HyClone) supplemented with 8% fetal bovine serum (HyClone), 1%

penicillin–streptomycin–fungizone (Lonza BioWhittaker), and 2 mM GlutaMAX (Gibco). Cells were grown in a humidified incubation chamber at 5% CO_2 and 37 °C. Cell line authenticity was verified by analysis of short tandem repeats (IDEXX Bioanalytics) and lines were determined mycoplasma free by PlasmoTest (InvivoGen).

Orthotopic bladder xenografts and dacomitinib treatment

NOD.*Cg-Prkdc*^{scid}*Il2rg*^{tm1Wjl}/SzJ (NSG™) mice were obtained from the Unit for Laboratory Animal Medicine Breeding Colony at the University of Michigan. Female NSG mice between the age of 3 to 6 months were given orthotopic bladder xenografts as previously described (PMID: 30683938).[6] One week after xenograft implantation, a group of female mice (N = 4) were given nine doses of dacomitinib by oral gavage at 15 mg kg^{-1} approximately every other day for three weeks. To measure bioluminescent signal, mice were given an IP injection of 3 mg D-luciferin (Regis Technologies) and after 10 minutes, signals were measured using an IVIS 200 Spectrum (Perkin Elmer). Bioluminescent signals coming from the bladder were measured by setting the minimum counts to 600 and using Living Image's "Auto ROI" feature with a 25% threshold. Mice were euthanized after 4 weeks post-xenograft-implantation.

Ethical considerations

All animal studies were conducted under protocols (PRO00007073) approved by the University of Michigan Institutional Animal Care and Use Committee (IACUC). The animal studies were conducted in compliance with the University of Michigan guidelines and federal regulations.

Urine collection

Mice were placed in a sterile empty cage without bedding. The cages were checked for urine in 10 minute intervals for a maximum of 30 minutes. Urine was immediately transferred to centrifuge tubes on ice and then stored at 4 °C throughout the day (until at least 50 μL of urine was collected). If insufficient urine was collected, the process was repeated approximately 2 hours later.

Pre-ELISA treatment of urine

Urine samples were spun for 30 seconds with 10 000 × g to remove the insoluble fractions in the urine. The supernatant was collected with clean microcentrifuge tubes and the pellets were discarded. The centrifuged urine samples were stored at 4 °C before taking ELISA measurements. The storing periods were typically less than three days.

Western blotting

Cells were washed with PBS, harvested by cell scraping, and then pelleted by centrifugation at 4 °C, 9300 × g for 5 minutes. Cell pellets were frozen at −80 °C. These pellets were then lysed in RIPA buffer (PMID: 18434311 (ref. 57)) for 1 hour on ice with intermittent vortexing. The lysed cells were then centrifuged at 4 °C, 13 200 × g for 8 minutes, supernatants were collected and quantified with the Bradford protein assay (Bio-Rad).[57] Gel electrophoresis was performed using equal amounts of protein on 4–20% Tris-Glycine gels, WedgeWell format (Novex). A wet transfer was used to move proteins from the gel to an Immobilon-FL PVDF membrane (Millipore), blocked with non-fat dry milk, and then incubated with primary antibody overnight at 4 °C followed by 1 hour at room temperature. The primary antibodies were anti-ADAM15 (NovoPro, 101503), anti-EGFR (ThermoFisher Scientific, H9B4), anti-GAPDH (Invitrogen, GA1R), anti-HER2 (Abcam, EP1045Y), and anti-Survivin (R&D Systems, 91630). Fluorescent secondary antibodies included IRDye 680LT goat anti-mouse and IRDye 800CW goat anti-rabbit (LI-COR). Blots were scanned using the Odyssey CLx (LI-COR) and analyzed using Image Studio v3.1.

Microfluidic ELISA system

The layout of the microfluidic ELISA system can be found in our previous publication.[29] Briefly, 12-channel polystyrene capillaries were used as the ELISA reactors. A CMOS camera was used to quantify the chemiluminescent signal of the ELISA reaction. A detailed and updated protocol for the microfluidic ELISA (applicable for all four biomarkers) that was used in this project can be found in the "Experimental" section.

ELISA reagents

The ELISA kits for human EGFR, HER2, ADAM15, and Survivin were all purchased from R&D systems. The catalog numbers are DY231(EGFR), DY1129B(HER2), DY935(ADAM15) and DYC647-5(Survivin), respectively. Note that the kits for EGFR and ADAM15 recognize the extracellular domains of the respective targeting proteins. The working solutions of the antibodies were prepared at the following concentrations: 4 μg mL^{-1} for EGFR capture antibody, 1 μg mL^{-1} for EGFR detection antibody, 10 μg mL^{-1} for HER2 capture antibody, 0.5 μg mL^{-1} for HER2 detection antibody, 20 μg mL^{-1} for ADAM15 capture antibody, 0.3 μg mL^{-1} for ADAM15 detection antibody, 2 μg mL^{-1} for Survivin capture antibody and 0.72 μg mL^{-1} for Survivin detection antibody. The working solutions of all capture antibodies were prepared with 1× PBS and the working solutions for all detection antibodies were prepared with 1× reagent diluent.

The ELISA coating buffer (1× PBS, DY006), concentrated wash buffer (WA126), concentrated streptavidin regular-HRP (DY998) and concentrated reagent diluent (10% BSA in 10× PBS, DY995) were purchased from R&D Systems. The working solution of the wash buffer and reagent diluent were diluted with Milli-Q water (R = 18.2 Ω) to achieve 1× working concentration (based on user's manual). The Superblock PBS buffer (ThermoFisher, 37518), the streptavidin poly-HRP stock solution (ThermoFisher, 21140) and the poly-HRP dilution buffer (1% casein in 1x PBS, ThermoFisher, N500)

were purchased from Thermo Fisher. The working solution of the streptavidin regular-HRP was prepared by diluting the stock solution 200 times with the reagent diluent working solution (1% BSA in 1× PBS). The working solution for the streptavidin poly-HRP was prepared by diluting the stock solution 1250 times with the poly-HRP dilution buffer. The chemiluminescent substrate (SuperSignal ELISA Femto Substrate, ThermoFisher, 37075) was used for detection. The working substrate solution was prepared by equal-volumetric mixing of the luminol + enhancer Solution and the Stable Peroxide Solution (all contained in the substrate kit) at room temperature.

PCA analysis procedure

To reduce dimensionality for classification we applied PCA analysis on the EGFR, HER2, ADAM15, and Survivin concentration results (measured with microfluidic ELISA). A natural logarithmic operation was first applied to all ELISA measurements. Then the measurements results were splinted into a training set (49 samples, including urine measurements from the low number group and a few additional baseline readings) and a testing set (34 samples). PCA was first applied to the 49-by-4 dataset to produce 49-by-4 principal component scores. Based on the eigenvalue, approximately 93% variability was explained with the first two PCs. Hence, we used the primary two principal components for further analysis. With the 4-by-4 PCA coefficients acquired from the training set, the PC scores of the testing set can be calculated by multiplying the PCA coefficients to the testing samples' dataset.

Conflicts of interest

The authors declare the following competing financial interest(s): M. K. K. O. and X. F. are co-founders of and have an equity interest in Optofluidic Bioassay, LLC.

Acknowledgements

The authors acknowledge the support from National Science Foundation under ECCS-1607250 and DBI-1451127.

References

1 R. L. Siegel, K. D. Miller and A. Jemal, Cancer statistics, 2018, *Ca-Cancer J. Clin.*, 2018, **68**, 7–30.
2 R. L. Siegel, K. D. Miller and A. Jemal, Cancer statistics, 2019, *Ca-Cancer J. Clin.*, 2019, **69**, 7–34.
3 S. M. Cohen, T. Ohnishi, L. L. Arnold and X. C. Le, Arsenic-induced bladder cancer in an animal model, *Toxicol. Appl. Pharmacol.*, 2007, **222**, 258–263.
4 B. Tian, Z. Wang, Y. Zhao, D. Wang, Y. Li, L. Ma, X. Li, J. Li, N. Xiao and J. Tian, Effects of curcumin on bladder cancer cells and development of urothelial tumors in a rat bladder carcinogenesis model, *Cancer Lett.*, 2008, **264**, 299–308.
5 A. Richmond and Y. Su, *Mouse xenograft models vs GEM models for human cancer therapeutics*, The Company of Biologists Ltd, 2008.
6 G. L. Hiles, A. L. Cates, L. El-Sawy, K. C. Day, L. J. Broses, A. L. Han, H. L. Briggs, A. Emamdjomeh, A. Chou and E. V. Abel, A surgical orthotopic approach for studying the invasive progression of human bladder cancer, *Nat. Protoc.*, 2019, **14**, 738.
7 R. Ito, T. Takahashi, I. Katano and M. Ito, Current advances in humanized mouse models, *Cell. Mol. Immunol.*, 2012, **9**, 208.
8 J. C. Garrison, T. L. Rold, G. L. Sieckman, S. D. Figueroa, W. A. Volkert, S. S. Jurisson and T. J. Hoffman, In vivo evaluation and small-animal PET/CT of a prostate cancer mouse model using 64Cu bombesin analogs: side-by-side comparison of the CB-TE2A and DOTA chelation systems, *J. Nucl. Med.*, 2007, **48**, 1327–1337.
9 C. M. Deroose, A. De, A. M. Loening, P. L. Chow, P. Ray, A. F. Chatziioannou and S. S. Gambhir, Multimodality imaging of tumor xenografts and metastases in mice with combined small-animal PET, small-animal CT, and bioluminescence imaging, *J. Nucl. Med.*, 2007, **48**, 295–303.
10 E. Chan, A. Patel, W. Heston and W. Larchian, Mouse orthotopic models for bladder cancer research, *BJU Int.*, 2009, **104**, 1286–1291.
11 W. Jäger, I. Moskalev, C. Janssen, T. Hayashi, S. Awrey, K. M. Gust, A. I. So, K. Zhang, L. Fazli and E. Li, Ultrasound-guided intramural inoculation of orthotopic bladder cancer xenografts: a novel high-precision approach, *PLoS One*, 2013, **8**, e59536.
12 S. Kuroda, T. Kubota, K. Aoyama, S. Kikuchi, H. Tazawa, M. Nishizaki, S. Kagawa and T. Fujiwara, Establishment of a non-invasive semi-quantitative bioluminescent imaging method for monitoring of an orthotopic esophageal cancer mouse model, *PLoS One*, 2014, **9**, e114562.
13 M. Keyaerts, V. Caveliers and T. Lahoutte, Bioluminescence imaging: looking beyond the light, *Trends Mol. Med.*, 2012, **18**, 164–172.
14 A. Sun, L. Hou, T. Prugpichailers, J. Dunkel, M. A. Kalani, X. Chen, M. Y. S. Kalani and V. Tse, Firefly Luciferase–Based Dynamic Bioluminescence Imaging: A Noninvasive Technique to Assess Tumor Angiogenesis, *Neurosurgery*, 2010, **66**, 751–757.
15 B. W. Van Rhijn, H. G. van Der Poel and T. H. van Der Kwast, Urine markers for bladder cancer surveillance: a systematic review, *Eur. Urol.*, 2005, **47**, 736–748.
16 O. P. Vrooman and J. A. Witjes, Urinary markers in bladder cancer, *Eur. Urol.*, 2008, **53**, 909–916.
17 M. Hanke, K. Hoefig, H. Merz, A. C. Feller, I. Kausch, D. Jocham, J. M. Warnecke and G. Sczakiel, A robust methodology to study urine microRNA as tumor marker: microRNA-126 and microRNA-182 are related to urinary bladder cancer, *Urol. Oncol.: Semin. Orig. Invest.*, 2010, **28**(6), 655–661.
18 S. D. Smith, M. A. Wheeler, J. Plescia, J. W. Colberg, R. M. Weiss and D. C. Altieri, Urine detection of survivin and diagnosis of bladder cancer, *JAMA, J. Am. Med. Assoc.*, 2001, **285**, 324–328.
19 X. Tan, M. K. Khaing Oo, Y. Gong, Y. Li, H. Zhu and X. Fan, Glass capillary based microfluidic ELISA for rapid diagnostics, *Analyst*, 2017, **142**, 2378–2385.

20 I. Jolliffe, *Principal component analysis*, Springer, 2011.

21 S. Tamura, Y. Wang, B. Veeneman, D. Hovelson, A. Bankhead III, L. J. Broses, G. Lorenzatti Hiles, M. Liebert, J. R. Rubin and K. C. Day, Molecular correlates of in vitro responses to dacomitinib and afatinib in bladder cancer, *Bladder Cancer*, 2018, **4**, 77–90.

22 R. Nicholson, J. Gee and M. Harper, EGFR and cancer prognosis, *Eur. J. Cancer*, 2001, **37**, 9–15.

23 N.-H. Chow, H.-S. Liu, E. Lee, C.-J. Chang, S.-H. Chan, H. L. Cheng, T. S. Tzai and J. Lin, Significance of urinary epidermal growth factor and its receptor expression in human bladder cancer, *Anticancer Res.*, 1997, **17**, 1293–1296.

24 M. Lae, J. Couturier, S. Oudard, F. Radvanyi, P. Beuzeboc and A. Vieillefond, Assessing HER2 gene amplification as a potential target for therapy in invasive urothelial bladder cancer with a standardized methodology: results in 1005 patients, *Ann. Oncol.*, 2009, **21**, 815–819.

25 S. Krüger, G. Weitsch, H. Büttner, A. Matthiensen, T. Böhmer, T. Marquardt, F. Sayk, A. C. Feller and A. Böhle, HER2 overexpression in muscle-invasive urothelial carcinoma of the bladder: Prognostic implications, *Int. J. Cancer*, 2002, **102**, 514–518.

26 N. Lucas, A. J. Najy and M. L. Day, The therapeutic potential of ADAM15, *Curr. Pharm. Des.*, 2009, **15**, 2311–2318.

27 G. L. Hiles, A. Bucheit, J. R. Rubin, A. Hayward, A. L. Cates, K. C. Day, L. El-Sawy, L. P. Kunju, S. Daignault, C. T. Lee and M. L. Day, ADAM15 is functionally associated with the metastatic progression of human bladder cancer, *PLoS One*, 2016, **11**, e0150138.

28 S. F. Shariat, R. Casella, S. M. Khoddami, G. Hernandez, T. Sulser, T. C. Gasser and S. P. Lerner, Urine detection of survivin is a sensitive marker for the noninvasive diagnosis of bladder cancer, *J. Urol.*, 2004, **171**, 626–630.

29 X. Tan, A. David, J. Day, H. Tang, E. R. Dixon, H. Zhu, Y.-C. Chen, M. K. Khaing Oo, A. Shikanov and X. Fan, Rapid Mouse Follicle Stimulating Hormone Quantification and Estrus Cycle Analysis Using an Automated Microfluidic Chemiluminescent ELISA System, *ACS Sens.*, 2018, **3**, 2327–2334.

30 D. H. Hovelson, A. M. Udager, A. S. McDaniel, P. Grivas, P. Palmbos, S. Tamura, L. L. de la Vega, G. Palapattu, B. Veeneman and L. El-Sawy, Targeted DNA and RNA sequencing of paired urothelial and squamous bladder cancers reveals discordant genomic and transcriptomic events and unique therapeutic implications, *Eur. Urol.*, 2018, **74**, 741–753.

31 I. Ojeda, M. Moreno-Guzmán, A. González-Cortés, P. Yáñez-Sedeño and J. Pingarrón, Electrochemical magnetoimmunosensor for the ultrasensitive determination of interleukin-6 in saliva and urine using poly-HRP streptavidin conjugates as labels for signal amplification, *Anal. Bioanal. Chem.*, 2014, **406**, 6363–6371.

32 Y. Wen, G. Liu, H. Pei, L. Li, Q. Xu, W. Liang, Y. Li, L. Xu, S. Ren and C. Fan, DNA nanostructure-based ultrasensitive electrochemical microRNA biosensor, *Methods*, 2013, **64**, 276–282.

33 O. Attrée, V. Guglielmo-Viret, V. Gros and P. Thullier, Development and comparison of two immunoassay formats for rapid detection of botulinum neurotoxin type A, *J. Immunol. Methods*, 2007, **325**, 78–87.

34 https://www.rndsystems.com/products/human-egfr-duoset-elisa_dy231.

35 https://www.rndsystems.com/products/human-erbb2-her2-duoset-elisa_dy1129b.

36 https://www.rndsystems.com/products/human-adam15-duoset-elisa_dy935.

37 https://www.rndsystems.com/products/human-total-survivin-duoset-ic-elisa_dyc647-2.

38 M. Shirley, Dacomitinib: first global approval, *Drugs*, 2018, **78**, 1947–1953.

39 P. D. Grivas, K. C. Day, A. Karatsinides, A. Paul, N. Shakir, I. Owainati, M. Liebert, L. P. Kunju, D. Thomas and M. Hussain, Evaluation of the antitumor activity of dacomitinib in models of human bladder cancer, *Mol. Med.*, 2013, **19**, 367–376.

40 H. Kawanishi, Y. Matsui, M. Ito, J. Watanabe, T. Takahashi, K. Nishizawa, H. Nishiyama, T. Kamoto, Y. Mikami and Y. Tanaka, Secreted CXCL1 is a potential mediator and marker of the tumor invasion of bladder cancer, *Clin. Cancer Res.*, 2008, **14**, 2579–2587.

41 D. Cappellen, C. De Oliveira, D. Ricol, S. de Medina, J. Bourdin, X. Sastre-Garau, D. Chopin, J. P. Thiery and F. Radvanyi, Frequent activating mutations of FGFR3 in human bladder and cervix carcinomas, *Nat. Genet.*, 1999, **23**, 18.

42 R. T. Bryan, H. L. Regan, S. J. Pirrie, A. J. Devall, K. Cheng, M. P. Zeegers, N. D. James, M. A. Knowles and D. G. Ward, Protein shedding in urothelial bladder cancer: prognostic implications of soluble urinary EGFR and EpCAM, *Br. J. Cancer*, 2015, **112**, 1052.

43 R. Bryan, N. Shimwell, W. Wei, A. Devall, S. Pirrie, N. James, M. Zeegers, K. Cheng, A. Martin and D. Ward, Urinary EpCAM in urothelial bladder cancer patients: characterisation and evaluation of biomarker potential, *Br. J. Cancer*, 2014, **110**, 679.

44 C.-x. Pan, H. Zhang, C. G. Tepper, T.-y. Lin, R. R. Davis, J. Keck, P. M. Ghosh, P. Gill, S. Airhart and C. Bult, Development and characterization of bladder cancer patient-derived xenografts for molecularly guided targeted therapy, *PLoS One*, 2015, **10**, e0134346.

45 T.-Y. Lin, Y. Li, Q. Liu, J.-L. Chen, H. Zhang, D. Lac, H. Zhang, K. W. Ferrara, S. Wachsmann-Hogiu and T. Li, Novel theranostic nanoporphyrins for photodynamic diagnosis and trimodal therapy for bladder cancer, *Biomaterials*, 2016, **104**, 339–351.

46 J. J. Morrissey, A. N. London, J. Luo and E. D. Kharasch, Urinary biomarkers for the early diagnosis of kidney cancer, *Mayo Clin. Proc.*, 2010, **85**, 413–421.

47 W. K. Han, A. Alinani, C.-L. Wu, D. Michaelson, M. Loda, F. J. McGovern, R. Thadhani and J. V. Bonventre, Human kidney injury molecule-1 is a tissue and urinary tumor marker of renal cell carcinoma, *J. Am. Soc. Nephrol.*, 2005, **16**, 1126–1134.

48 J. Groskopf, S. M. Aubin, I. L. Deras, A. Blase, S. Bodrug, C. Clark, S. Brentano, J. Mathis, J. Pham and T. Meyer, APTIMA PCA3 molecular urine test: development of a method to aid in the diagnosis of prostate cancer, *Clin. Chem.*, 2006, **52**, 1089–1095.

49 P. J. Mitchell, J. Welton, J. Staffurth, M. D. Mason, Z. Tabi and A. Clayton, Can urinary exosomes act as treatment response markers in prostate cancer?, *J. Transl. Med.*, 2009, **7**, 4.

50 P. Gontero, S. Banisadr, B. Frea and M. Brausi, Metastasis markers in bladder cancer: a review of the literature and clinical considerations, *Eur. Urol.*, 2004, **46**, 296–311.

51 M. A. Knowles and C. D. Hurst, Molecular biology of bladder cancer: new insights into pathogenesis and clinical diversity, *Nat. Rev. Cancer*, 2015, **15**, 25–41.

52 T. Szarvas, M. Becker, F. Vom Dorp, C. Gethmann, M. Tötsch, Á. Bánkfalvi, K. W. Schmid, I. Romics, H. Rübben and S. Ergün, Matrix metalloproteinase-7 as a marker of metastasis and predictor of poor survival in bladder cancer, *Cancer Sci.*, 2010, **101**, 1300–1308.

53 A.-R. Scheffer, S. Holdenrieder, G. Kristiansen, A. von Ruecker, S. C. Müller and J. Ellinger, Circulating microRNAs in serum: novel biomarkers for patients with bladder cancer?, *World J. Urol.*, 2014, **32**, 353–358.

54 S. L. Wood, M. A. Knowles, D. Thompson, P. J. Selby and R. E. Banks, Proteomic studies of urinary biomarkers for prostate, bladder and kidney cancers, *Nat. Rev. Urol.*, 2013, **10**, 206.

55 S. Eissa, H. Habib, E. Ali and Y. Kotb, Evaluation of urinary miRNA-96 as a potential biomarker for bladder cancer diagnosis, *Med. Oncol.*, 2015, **32**, 413.

56 X. M. Piao, P. Jeong, Y. H. Kim, Y. J. Byun, Y. Xu, H. W. Kang, Y. S. Ha, W. T. Kim, J. Y. Lee and S. H. Woo, Urinary cell-free microRNA biomarker could discriminate bladder cancer from benign hematuria, *Int. J. Cancer*, 2019, **144**, 380–388.

57 A. J. Najy, K. C. Day and M. L. Day, The ectodomain shedding of E-cadherin by ADAM15 supports ErbB receptor activation, *J. Biol. Chem.*, 2008, **283**, 18393–18401.

